Biology and Fertility of Soils (2024) 60:1143–1157
https://doi.org/10.1007/s00374-024-01862-5

ORIGINAL PAPER

An innovative soil mesocosm system for studying the effect of soil moisture and background NO on soil surface C and N trace gas fluxes

Logapragasan Subramaniam[1] · Florian Engelsberger[1] · Benjamin Wolf[1] · Nicolas Brüggemann[2] · Laurent Philippot[3] · Michael Dannenmann[1] · Klaus Butterbach-Bahl[1,4]

Received: 16 April 2024 / Revised: 25 August 2024 / Accepted: 31 August 2024 / Published online: 18 September 2024

Abstract

Nitric oxide (NO) is a key substance in atmospheric chemistry, influencing the formation and destruction of tropospheric ozone and the atmosphere's oxidizing capacity. It also affects the physiological functions of organisms. NO is produced, consumed, and emitted by soils, the effects of soil NO concentrations on microbial C and N cycling and associated trace gas fluxes remain largely unclear. This study describes a new automated 12-chamber soil mesocosm system that dynamically changes incoming airflow composition. It was used to investigate how varying NO concentrations affect soil microbial C and N cycling and associated trace gas fluxes under different moisture conditions (30% and 50% WFPS). Based on detection limits for NO, NO_2, N_2O, and CH_4 fluxes of < 0.5 µg N or C m^{-2} h^{-1} and for CO_2 fluxes of < 1.2 mg C m^{-2} h^{-1}, we found that soil CO_2, CH_4, NO, NO_2, and N_2O were significantly affected by different soil moisture levels. After 17 days cumulative fluxes at 50% WFPS increased by 40, 400, and 500% for CO_2, N_2O, and CH_4, respectively, when compared to 30% WFPS. However, cumulative fluxes for NO, and NO_2, decreased by 70, and 40%, respectively, at 50% WFPS when compared to 30% WFPS. Different NO concentrations tended to decrease soil C and N fluxes by about 10–20%. However, with the observed variability among individual soil mesocosms and minor fluxes change. In conclusion, the developed system effectively investigates how and to what extent soil NO concentrations affect soil processes and potential plant–microbe interactions in the rhizosphere.

Keywords Automated soil mesocosms system · N and C trace gases · Nitric oxide effects

Introduction

Nitric oxide (NO) has unique chemical properties and is involved in a variety of biological functions in both prokaryotes and eukaryotes (Ma et al. 2020; Medinets et al. 2015). In plants, NO is considered an important physiological mediator involved in various processes such as root growth, stomatal closure, flowering, iron homeostasis, immunity, and responses to abiotic stresses (Wendehenne et al. 2014; Yu et al. 2014). It acts as a signaling molecule in cellular processes and modulates the production/mobilization of secondary messengers and reactive oxygen species, the activity of proteins through post-translational modifications, and the expression of numerous genes regulating microbial and plant processes (Gaupels et al. 2011; Jeandroz et al. 2013; Medinets et al. 2015).

In addition, NO also has diverse effects on soil microbes. Previous work has shown that microorganisms use various transcriptional regulators to sense NO (Koul et al. 2015). Biochemical evidence that NO itself interacts with bacterial regulatory proteins has been reported in the case of SoxR, FNR, NorR, NosR, and FixK, transcriptional regulators involved in oxidative stress response, anaerobic metabolism, NO detoxification, respiratory reduction of N_2O, and nitrogen fixation, respectively (Spiro 2007). Thus, NO plays

✉ Klaus Butterbach-Bahl
klaus.butterbach-bahl@kit.edu

1 Institute for Meteorology and Climate Research Atmospheric Environmental Research (IMK-IFU), Division "Terrestrial Bio-Geo-Chemistry", Karlsruhe Institute of Technology (KIT), Kreuzeckbahnstr. 19, 82467 Garmisch-Partenkirchen, Germany

2 Institute of Bio- and Geosciences, Agrosphere (IBG-3), Forschungszentrum Jülich GmbH, 52428 Jülich, Germany

3 University of Bourgogne, INRAE, Institut Agro Dijon, AgroecologieUniversity of Bourgogne, INRAE, Institut Agro Dijon, Agroecologie, 17 Rue Sully, 21000 Dijon, France

4 Center for Landscape Research in Sustainable Agricultural Futures - Land-CRAFT, Department of Agroecology, Aarhus University, Ole Worms Allé 3, 8000 Aarhus C, Denmark

an important role in the regulation of numerous microbial functions, such as protection against antibiotics and oxidative stress (Gusarov et al. 2009), adaptation to anaerobic conditions, biofilm formation, and motility (Arruebarrena Di Palma et al. 2013; Medinets et al. 2015). However, these regulatory effects of NO have mostly been studied at the population level in vitro, and therefore little is known about the response of microbial communities to NO in complex environments such as soils. It is also speculated that NO affects not only microbial N metabolism but also mineralization of organic matter in soils (Pilegaard 2013; Schuster and Conrad 1992), the latter has, to our knowledge, never been studied. At higher concentrations, NO can induce both nitrosative and oxidative damage with numerous toxic effects on bacteria, including direct modification of membrane proteins, lipid peroxidation, and DNA cleavage (Privett et al. 2012). However, pure culture studies have shown that some bacteria are more susceptible to NO than others (Schairer et al. 2012). This antimicrobial effect of exogenous NO application has mostly been studied in medical research, but rarely in complex ecosystems and never in soil.

Understanding how exogenous NO may affect soil microbial processes and soil-atmosphere exchange processes requires accurate measurements of trace gas fluxes (Harazono et al. 2015). However, research on the effects of NO on soil microbial processes has been hampered, in part, by the lack of mesocosm systems that allow background NO concentrations to be varied while also allowing the soil-atmosphere exchange of other trace gases to be measured.

Therefore, we designed a novel mesocosm system that allows for dynamic changes in background NO concentrations while simultaneously allowing for high temporal resolution measurements of soil CO_2, CH_4, NO, NO_2, and N_2O fluxes. We hypothesized that at elevated NO concentrations, microbial activity, as measured by soil respiration fluxes, would be negatively affected. In addition, we speculated that NO would also negatively affect all other measured trace gas fluxes due to a decrease in microbial activity, although to varying degrees depending on soil moisture, which is known to be a major environmental factor affecting microbial processes and microbial activity.

Material and methods

The construction of the mesocosm system was carried out at the laboratory of the Institute for Meteorology and Climate Research Atmospheric Environmental Research (IMK-IFU), KIT Campus Alpin (N 47° 28′ 37.2606", E 11° 3′ 47.484") in Garmisch-Partenkirchen, Germany.

To study the effect of varying soil or headspace NO concentrations on soil microbial activity and soil-atmosphere exchange, we defined several key requirements:

a) Automated control of gas flow and sampling for 12 mesocosms;
b) Provision of inlet gas sample air by either headspace flushing or soil purge air;
c) Automated on-line detection and recording of inlet and outlet gas concentrations;
d) Multiple flux measurements per day for each soil mesocosm;
e) Temperature and light control (for plant-soil mesocosm experiments);
f) High sensitivity of flux measurements;
g) Structured data streams for automated flux calculations and visualization.

Based on these requirements we designed a fully automated 12-chamber soil mesocosm system (see Fig. 1), where the soil mesocosms were placed in a thermostatic cabinet. The 12 soil mesocosms could be continuously and independently flushed with ambient air from a pressurized air buffer tank and sets of six could be spiked with different NO concentrations. Solenoid valves were used to facilitate individual soil or headspace flushing, and airflow from the inlet to the analyzers was directly controlled by mass flow controllers (MFCs). Outflow air from each soil mesocosm was directed by a multi-position valve to a high-precision multi-gas analyzer (MIRO, analytical, MGA9 series, Switzerland) that continuously measures gas concentrations of NO, NO_2, N_2O, NH_3, CO_2, CO, CH_4, and H_2O with 1-second time resolution. The resulting data were used to calculate gas fluxes under specified soil environmental conditions and NO headspace/soil air concentrations.

Soil mesocosm system

For the soil mesocosm system, cylindrical Plexiglas cuvettes (internal Ø: 126.5 mm, inner height: 200 mm; polymethylmethacrylate material; SAHLBERG GmbH and Co. KG, Germany) were used. In total, the soil mesocosm system consisted of 12 soil mesocosms plus an empty mesocosm used as a reference chamber.

The individual soil mesocosms were tightly sealed with two removable lids at the top and bottom, secured with a custom aluminum U-frame and stainless-steel clip lock. A rubber O-ring was used around the lid to ensure airtightness. The top cover was designed with an inlet (inner Ø: 3 mm) and an outlet (inner Ø: 1.5 mm). An LED light (Bioledex LED module, Ø60 mm, 24 V, 9 W, 3500 K) was positioned inside the lid wall to act as a light source if plants are cultivated inside the mesocosm. The light emitted by the LED had a full spectrum for plant illumination, with a color temperature of 3500 K plus red. The wavelengths covered a range from 410 to 710 nm, the full spectrum required for optimal plant growth and development (Hogewoning et al.

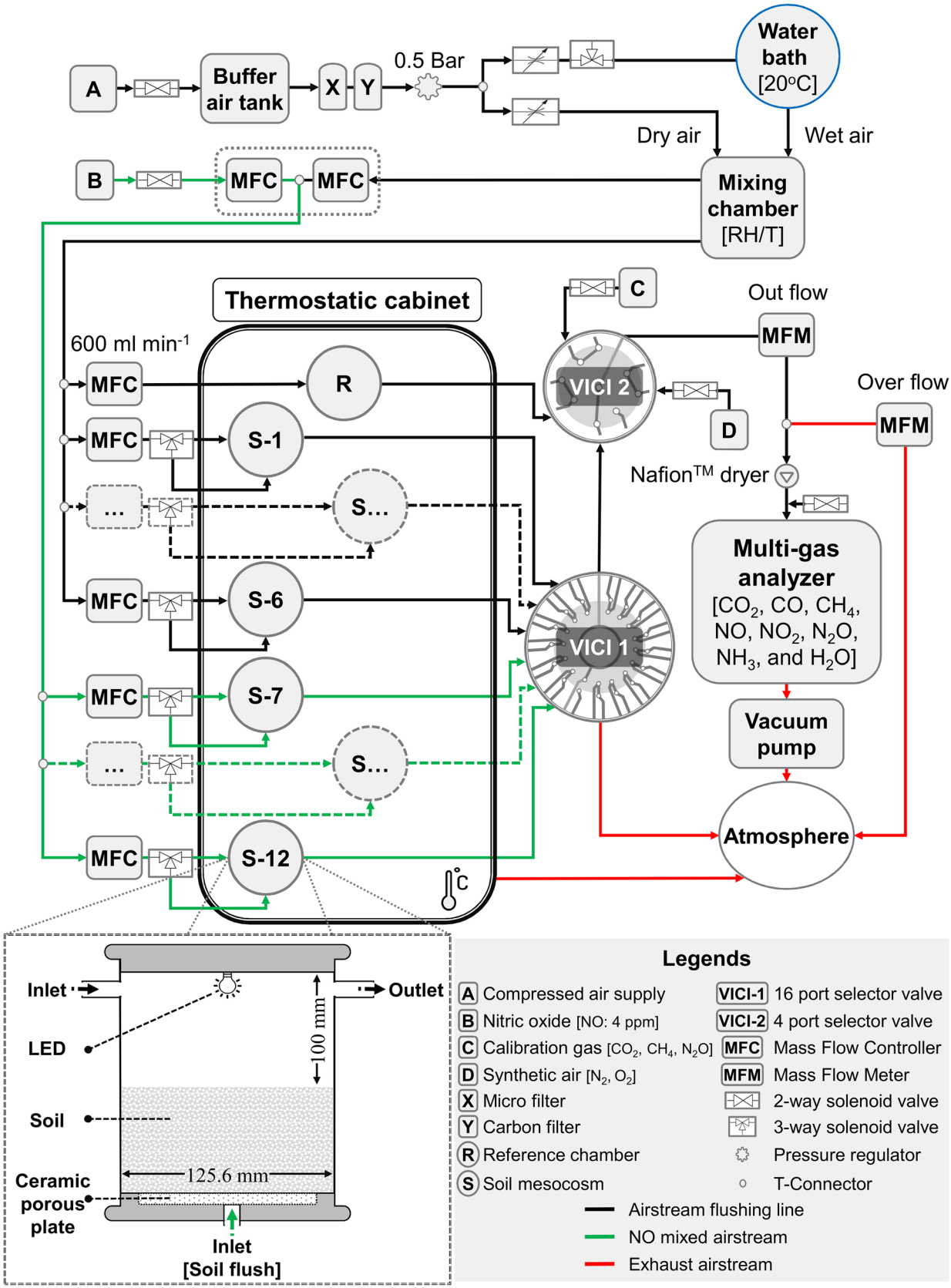

Fig. 1 Schematic flowchart and operational features of the fully automated soil mesocosm system

2012). The LED was powered by a stabilized power supply (model HEP-320-24A) that accepts input voltages of 100-240 V AC at 50/60 Hz and outputs 24 V DC at 13.34A. An LED dimmer (model CVDIM1 LED dimmer, 4 × (12–36) V and 4 × 5A) was used to control the light intensity. The bottom cover was designed with an inlet (inner Ø: 3 mm) to facilitate airflow through the bottom of the mesocosm. In addition, the bottom outlet can be used to collect leachate after simulated rainfall events.

All soil mesocosms were placed in a thermostatic cabinet (model ET 651–8; 395 L, Tintometer GmbH, Dortmund, Germany). Soil gas flux measurements were based on the dynamic chamber approach (Butterbach-Bahl et al. 1997), which requires constant flushing of individual soil mesocosms with a defined air stream. Therefore, fluxes were calculated from the difference between inlet and outlet concentrations and the total mass of airflow.

Soil mesocosm system airflows – general overview

The total air flow for flushing the soil mesocosms, either from the headspace only or from the bottom, was obtained from a pressurized air buffer tank (50 L, 8 bar; Fini Compressors, Bologne, Italy), which was filled from time to time with ambient outdoor air. Before being provided to the mesocosm systems, the air was filtered by a microfilter (5 µm particle filter; Futura Series FU 831, Riegler and Co. KG, Germany) and a carbon filter (Activated carbon filter; Futura Series FU 891, Riegler and Co. KG, Germany) to remove dust particles and noxious gases such as NO_x, respectively (Yu et al. 2008). It should also be noted that a pressure regulator (AIRTAC GR200-08 pressure regulator; Riegler and Co. KG, Germany) was used to reduce the downstream pressure of the buffer tank to 0.5 bar to avoid pressure deficits in the open dynamic chambers (Gao and Yates 1998). A dehumidifier was used to remove moisture from the outlet of the buffer tank. To re-humidify the air stream to the desired level, the inlet air stream was split into two air streams, one of which was bubbled through deionized water filled in a gas bubbler before finally rejoining the main air stream (Fig. 1). The humidity and temperature of the air stream were measured (RH/T probe HC2-S3C03, ROTRONIC Messgeräte GmbH, Germany). Subsequently, the re-humidified air stream was divided into two lines, one line was directly connected to block 1 of the mesocosm system (C1—C6), which normally received unspiked ambient air, while the other, block 2, of the mesocosm system (C7-C12), was additionally spiked with nitric oxide (NO) using an additional gas flow mass controller (Red-y smart series, Voegtlin instruments GmbH, Muttenz, Switzerland) to inject NO calibration gas with 4 ppm NO in synthetic air into the air stream. All airflow components within the mesocosm system were connected using PTFE tubing (polytetrafluoroethylene; ScanTube GmbH, Germany). Black PTFE tubing was chosen specifically to prevent light-induced oxidation of NO (Weber and Rennenberg 1996). A humidity sensor and a temperature sensor (Vaisala, Finland) were integrated into the system and positioned adjacent to the humidifier on the air stream that purged the mesocosms.

Soil mesocosm system airflows – technical specifications

For dynamic chamber measurements under steady-state conditions, the mixing ratio difference is inversely related to the airflow rate. At low airflow rates, there is a potential for diffusive flow from the enclosed soil matrix, which may result in an underestimation of the true trace gas flux. Conversely, at high airflow rates, the pressure deficit in the headspace of the soil mesocosm can affect the advective flux from the soil matrix, leading to an overestimation of the true flux (Gao and Yates 1998). Therefore, it is essential to optimize the airflow rate within the mesocosm system during incubation, taking into account the trade-off between several partially conflicting requirements, such as flux detection limit, time response, and changes in turbulence resistances (Pape et al. 2009). In this study, each mesocosm was constantly flushed at a rate of 600 ml min^{-1} and the flow was continuously monitored by mass flow controllers (MFCs; Bronkhorst High-Tech B.V., The Netherlands), and the airflow was evenly distributed to all soil mesocosms (Fig. 1). The ambient background airflow was displayed for visual observation (bright, wide angle, 1.8" display, Bronkhorst High-Tech B.V. Netherlands). The airflow from the MFCs was connected to a 3-way solenoid valve (3/2 way valve; model 137850, USA; Ham-Let GmbH, Germany) that could divert the airflow through either the headspace or soil depending on the defined gas sampling sequence. The outlet of each mesocosm was connected to a VICI-1 multi-position valve (VICI, 16 port SF flow-through multi-position valve, Germany) through an air particulate filter (SWAGELOK®, In-line particulate filter, Germany), which traps and retains finer particles (7 microns) that could damage the VICI valves. The inlets of VICI-1 were connected to mesocosms 1 to 12, and the outlet of VICI-1 was connected to the inlet of the multi-position valve VICI-2 (VICI, 4-port SF flow-through multi-position valve, Germany). Based on the defined gas sampling sequence, VICI-1 decides whether to divert the sample air to VICI-2, which is also connected to various gases such as reference air, zero gas (or synthetic air), and calibration gas. VICI -2 diverts the gas to the multi-gas analyzer according to the gas sampling sequence (Fig. 1). The sampling cycle began with zero air for 3 min in the first cycle and 2 min in the second cycle, followed by 6 min

of reference chamber air and 6 min of soil mesocosm air (Fig. S1). The average of the last 2 min of gas concentration during the steady-state condition was used for flux calculation, with calibration performed manually at the beginning of each experiment.

The total airflow leaving the mesocosm system was monitored by a mass flow meter (MFM; Bronkhorst High-Tech B.V., The Netherlands) located downstream of the VICI-2, and this information is used for post-flux calculations (Fig. 1).

Measurements of gas concentrations

A multi-gas analyzer (MIRO analytical, MGA9 series, Switzerland) was used to measure the gas concentrations of the air streams. The sample airflow to the multi-gas analyzer is approximately 400 ml min^{-1} (or sccm), and this air flow is driven by a vacuum pump that also creates a vacuum in the measurement cells. Before entering the MIRO analyzer the air was dried with a Nafion™ dryer, known for its hygroscopic ion exchange properties (Yu et al. 2008), to reduce the water vapor content by around 90%. The MIRO instrument uses mid-infrared laser spectrometry based on direct laser absorption spectroscopy methods to provide highly sensitive and selective measurements. The MIRO instrument uses five mid-infrared quantum cascade lasers (QCLs) to simultaneously measure the concentrations of NO, NO_2, N_2O, CO_2, CH_4, and H_2O (NH_3, and CO, but not used here).

It should be noted, that gas concentration measurements by the MIRO analyzer are sensitive to pressure changes due to switching of valves from one soil mesocosm to the other or direct measurements of calibration gas or inlet gas concentrations. Therefore, to prevent any pressure difference in the system during the valve switching or system shutdown, a two-way solenoid valve (2/2 way valve; model 137850, USA; Ham-Let GmbH, Germany) was installed in the main line to the MIRO multi-gas analyzer. This valve automatically opens when switching or during system shutdown, allowing the MIRO to suck in air from the outside.

Control unit for the soil mesocosm system

The soil mesocosm system is computer-controlled with respect to inflow air volume and air/NO mixing ratio, temperature, pressure, humidity, air outflow and overflow (quality control), and control of solenoid valves to direct air flows.

The data acquisition software IDASw (Integrated Data Acquisition Software, (IMK-IFU), KIT, Garmisch-Partenkirchen, Germany) was used as the main operating software for the soil mesocosm system. IDASw uses a pre-prepared configuration file containing information about the gas sampling sequence, specifying the period and number of mesocosms to be sampled at specific time intervals. The data acquisition and control use a set of modules (ICP DAS-EUROPE GmbH) consisting of a bus module and three other digital input/output and analog modules. The digital input/output and analog modules (i-7061, i-7060D, and i-7019R) provide digital input/relay output and analog input/digital for reading out sensors such as combined humidity/temperature probes or for controlling gas flows through the mass flow controllers or valves, respectively. In general, all gas flows and sensors are controlled by the software via the ICP modules, except for the gas concentration measurements, which run on the MIRO multi-gas analyzer, with data stored independently. However, both computers were synchronized to a common time server using Tardis 2000 software.

Calculation of trace gas fluxes

For the calculation of trace gas fluxes from individual soil mesocosms using a dynamic chamber approach, we assumed that a) the soil-atmosphere exchange is driven by diffusion due to a concentration gradient between the soil surface and the atmosphere, b) the headspace air of the mesocosms is well mixed, and that possible surface reactions of reactive trace gases, especially NO, can be neglected because O_3 concentrations in the incoming air stream are at the detection limit (< 10 ppbv) and because black Teflon tubes were used to connect the mesocosms to the analyzer (Butterbach-Bahl et al. 1997).

The trace gas fluxes between the soil matrix and mesocosm air are quantified by the mass balance of the enclosed chamber system (Gao and Yates 1998).

$$F_{tracegas} = \left(\frac{(Q \times 10^{-6} \times 60)}{A}\right) \cdot \left(\frac{(P \times (M \times 10^{6}))}{(R \times (T + 273.15))}\right) \cdot \left((\mu_{cham} - \mu_{amb}) \times 10^{-6}\right) \quad (1)$$

$F_{trace\ gas}$ Trace gas flux (µg (C or N) m^{-2} h^{-1})

Q Airflow (ml min^{-1})

A Enclosed chamber (soil) surface area (m^2)

R Universal (or Ideal) gas constant (8.206×10^{-5} m^3 atm K^{-1} mol^{-1})

T Temperature of the gas (°C)

P Pressure of the gas (atm)

M Molecular mass (g mol^{-1})

μ_{amb} Ambient or inflow air concentration (ppm or µmol mol^{-1})

μ_{Cham} Chamber or outflow air concentration (ppm or µmol mol^{-1})

The determination of trace gas concentration is commonly based on the molar ratio of the gas to the moist-air mixing ratio concerning dry air. However, the actual gas concentration is subject to dilution by water vapor present in the chamber volume of moist air. In dynamic chamber techniques, especially when working with moist soils, the concentration of water vapor continuously increases due to evapotranspiration from the plant-soil system or due to soil evaporation. Relative humidity can have a significant impact on the mixing ratio, with even a 1% change in relative humidity at an ambient temperature of 25 °C and relative humidity of 65% within the chamber resulting in a 20 ppm shift in mixing ratio (Harazono et al. 2015; Webb et al. 1980). To account for water vapor dilution, trace gas fluxes were adjusted to the dry basis using water vapor concentration data obtained by the MIRO multi-gas analyzer and the following formula (Eugster and Merbold 2015):

$$M_{dry} = \left(M_{wet}\right) \bullet \left(\frac{1}{1 - X_{water}}\right) \quad (2)$$

M_{dry} Trace gas concentration on a dry-air basis (ppm or µmol mol^{-1})

M_{wet} Trace gas concentration on a moist-air basis (ppm or µmol mol^{-1})

X_{water} Amount fraction of water vapor in the outflow air stream.

System response times and trace gas flux detection limits

To better understand the system response time to changes in headspace gas mixtures and to quantify the detection limits for trace gas fluxes, we performed tests with empty mesocosms. The system response time was measured for the time it took to reach stable gas concentrations after switching the headspace concentration of the mesocosms from ambient air to ambient air spiked with 400 ppbv NO and was approximately 90 s for empty mesocosms (Fig. 2).

The calculation of the detection limit of the trace gas fluxes was based on the comparison of the trace gas concentration measurements in block 1) (mesocosms 1–6) and block 2) (mesocosms 7–12) over a period of three days, while all mesocosms were continuously flushed with ambient air (Table 1).

Experiments with soils

For the soil experiment, topsoil (0–0.2 m) was obtained from an arable field at the research station CEREEP (Centre de Recherche en Ecologie Prédictive) in Saint-Pierre-les-Nemours, France (N 48°17′14.48″, E 2°40′34.64″). The soil is classified as cambisol (IUSS Working Group WRB 2022), with a total organic carbon content of 14.7 g kg^{-1}, total nitrogen content of 1.19 g kg^{-1}, a pH of 5.22 and a sandy loam texture (clay: 6.9%; silt: 19.0%; sand:74.1%). The soil was transported to the laboratory of IMK-IFU in December 2022, air-dried, sieved at 4 mm, and stored at 4 °C until used in the experiments.

For the experiment, the sieved soil was layered into the mesocosms in 2 cm increments, compressed to achieve a bulk density of 1.3 gcm^{-3}, and built up to a final depth of 10 cm. Here we report on two independent experiments conducted with two different soil moisture contents (30 and 50% WFPS), comparing soil-atmosphere trace gas fluxes for treatments with ($N = 6$) and without spiking the ambient air ($N = 6$) with approximately 400 ppbv NO, thereby referring to previous in-situ measurements of NO concentrations in a forest stand in South-West Germany (Medinets et al. 2019).

The Water Filled Pore Space (WFPS) was calculated as follows:

$$WFPS\ (\%) = \frac{Gravimetric\ water\ content\ (\%)}{Total\ porosity} \cdot Soil\ Bulk\ density \cdot 100 \quad (3)$$

where $Total\ porosity = 1 - \frac{Soil\ bulk\ density}{Particle\ density}$ (Assumption, 2.65 g cm^{-3} as particle density).

The schedule of the soil incubation experiment is outlined in Fig. 3

Statistical analysis

The collected data, including the VICI valve switching information from the control computer (IDASw), the flow rates observed by the mass flow meter (MFM), and the gas concentration measurements obtained by the multi-gas analyzer (MIRO), were pre-processed by a customized R script. This R script calculated fluxes based on the formulae provided (see above). A repeated-measures paired t-test, with a significance level (α) of 0.05, was used to identify the significant effects of elevated NO headspace concentrations on soil-atmosphere trace gas fluxes and to compare the cumulative fluxes of the observed soil-atmosphere exchange rates between control and NO-flushed soils.

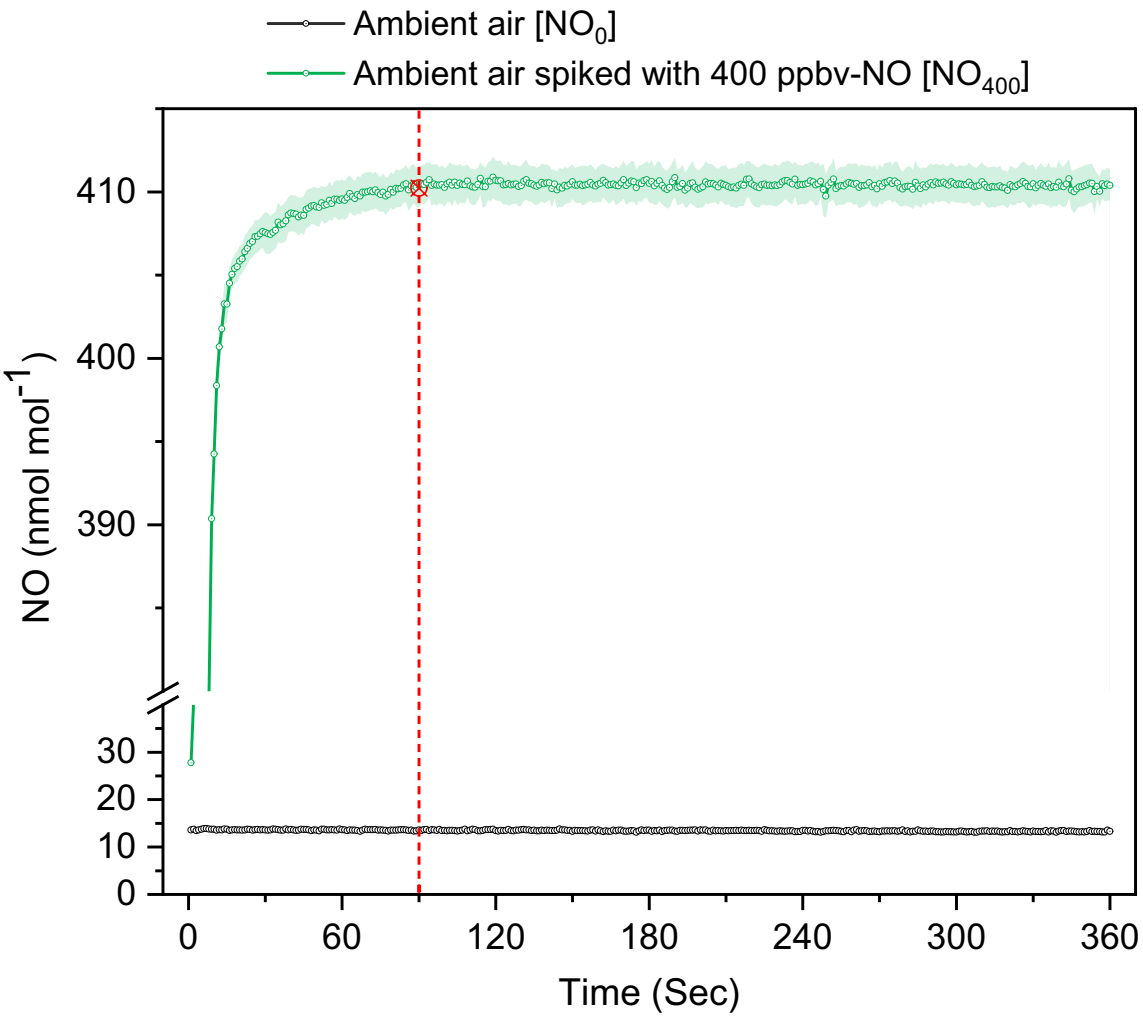

Fig. 2 Response time of the new mesocosm system to changes in headspace concentrations. Continuous measurements of NO concentrations at 1 s intervals are given. At time zero, a portion of the air stream was spiked with approximately 400 ppbv NO and directed to mesocosms 7–12 (block 2), while the other portion reflected the NO concentration measured in mesocosms 1–6 (block 1), which were flushed with ambient air only (background concentration 14 ppbv). Shown are mean ± SE values ($N = 6$)

Plots and graphs were generated using Origin(Pro), 2020b (OriginLab Corporation, Northampton, MA, USA).

Results

Effect of different NO concentrations in ambient air and soil moisture levels on soil CO_2 and CH_4 fluxes

Re-wetting of the air-dried soil to the target soil moisture levels of 30% or 50% WFPS resulted in large increases in soil respiration values from < 25 mg C m^{-2} h^{-1} to about 100 mg C m^{-2} h^{-1} after 24 h (Fig. 4). However, as the 3-day soil flushing period started on day 2 (either with NO-free (NO_0) or with ambient air spiked with 400 ppbv (NO_{400})), the peak of soil CO_2 emissions induced by soil re-wetting was not fully recorded. After the 3-day soil flushing period, CO_2 fluxes were < 50 mg C m^{-2} h^{-1} and were stimulated only slightly (50% WFPS) or not at all (30% WFPS) by the addition of N fertilizer (60 kg N ha^{-1}) on day 7. CO_2 fluxes after the second soil flushing period (days 9–11) stabilized at about the same level as at the end of day 8, i.e. around 30 mg C m^{-2} h^{-1} (30% WFPS) or 60 mg C m^{-2} h^{-1} (50% WFPS), revealing that re-wetting the soil to 50% WFPS significantly increased the soil CO_2 fluxes (see Fig. 4, Table 2).

Increasing NO concentrations in the ambient air stream to 400 ppbv NO (NO_{400}) tended to reduce soil CO_2 fluxes by > 10% for soils rewetted to 50% compared to NO_0, while the NO effect was weaker (5–10% to insignificant) for soils rewetted to 30% WFPS (see Table 2, Fig. 4).

Over the whole observation period and for soils re-wetted to 30% or 50% WFPS, CH_4 fluxes varied within a narrow

Table 1 Observed variations in observed trace gas concentrations in air samples taken from mesocosms of block 1 ($N=6$) as compared to mesocosms of block 2 (mean ± SD, $N=6$) while continuously purging the headspace of the mesocosms with ambient air over a period of three days

Trace gas	Concentration difference between mesocosm vessels of block 1) and 2)	Flux detection limit
	[ppmv or ppbv]	
NO	0.28 ppbv	0.05 ± 0.61 µg N m^{-2} h^{-1}
NO_2	0.03 ppbv	0.002 ± 0.042 µg N m^{-2} h^{-1}
N_2O	0.25 ppbv	0.38 ± 0.53 µg N m^{-2} h^{-1}
CO_2	0.21 ppmv	1.18 ± 1.21 mg C m^{-2} h^{-1}
CH_4	0.81 ppbv	0.06 ± 1.57 µg C m^{-2} h^{-1}

range of + 10 to -10 µg C m^{-2} h^{-1}. Neither re-wetting nor different soil moisture levels or different NO concentrations in the ambient air flow showed a significant effect on CH_4 fluxes (Fig. S2, Table 2).

Effect of different NO concentrations in ambient air and soil moisture levels on soil N (NO, NO_2, and N_2O) trace gas fluxes

In contrast to CO_2 fluxes, re-wetting of dried-out soils to target soil moisture levels of 30% or 50% WFPS didn't result in an immediate stimulation of soil NO fluxes. However, NO fluxes increased significantly after the first soil flushing period to values up to about 80 µg N m^{-2} h^{-1} for soils re-wetted to 30% WFPS and up to 10 µg N m^{-2} h^{-1} for soils re-wetted to 50% WFPS. Soil N fertilization on day 7 resulted in a period of high NO emissions for the 30% WFPS soil, while only a very short period of slightly elevated NO fluxes was observed for the 50% WFPS soil (see Fig. 5). NO fluxes after the second soil flushing period were rather constant in a range of about 60–90 µg N m^{-2} h^{-1} for soils at 30% WFPS and in a range of 30–50 µg N m^{-2} h^{-1} for soils at 50% WFPS. Over all measurement periods, soil NO fluxes were always significantly lower at 50% WFPS compared to 30% WFPS.

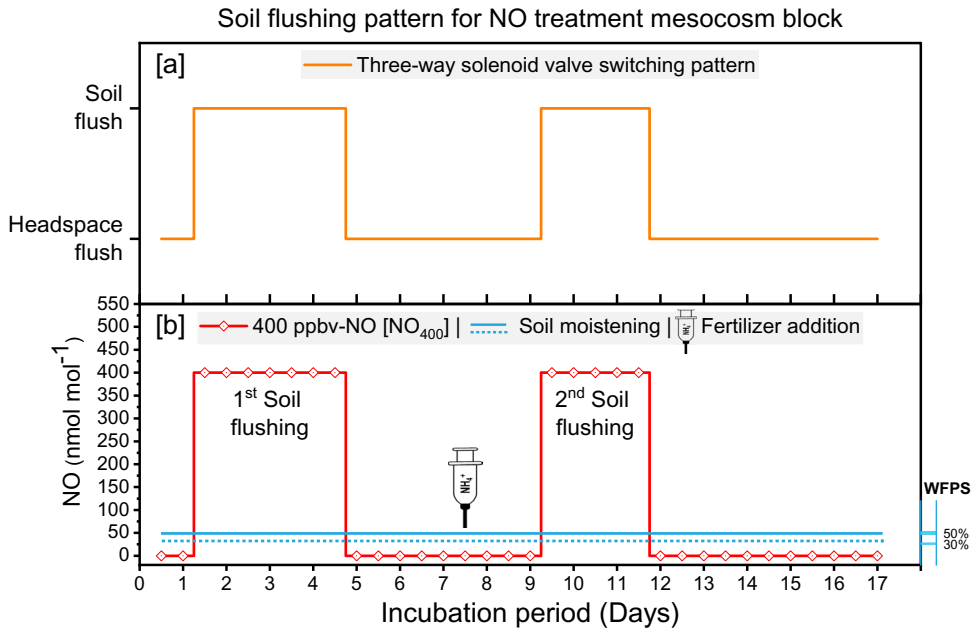

Fig. 3 Outline of the experimental design to investigate the effect of flushing soil and headspace air with different concentrations of NO (control [NO_0]: 0 ppbv, NO treatment [NO_{400}]: +400 ppbv, all in ambient air). On day 1, air-dried soil was added to the individual mesocosms (6 × control, 6x + 400 ppbv NO), compacted to the target bulk density (1.3 g cm^{-3}), and the soil was moistened in-situ to two different soil moisture levels (calculated as water-filled pore space): 30% in experiment (**a**) and 50% in experiment (**b**). On day 7, the soils received a simulated fertilizer N input of 60 kg N ha^{-1}. The corresponding amount of $(NH_4)_2SO_4$ was dissolved in distilled water and 12 ml of the solution was injected at a depth of 2 cm using a syringe with a side-port cannula. To effectively saturate the soil profile with a given NO concentration, soil flushing is preferred because it ensures effective distribution throughout the soil profile, unlike headspace flushing, which may only enrich the soil surface layer. In this study, we adjusted the timing of soil flushing to ensure that the target soil NO concentration was achieved throughout the soil profile. Note that the calculation of soil-atmosphere trace gas fluxes was performed only during periods of headspace flushing and not during periods of soil flushing

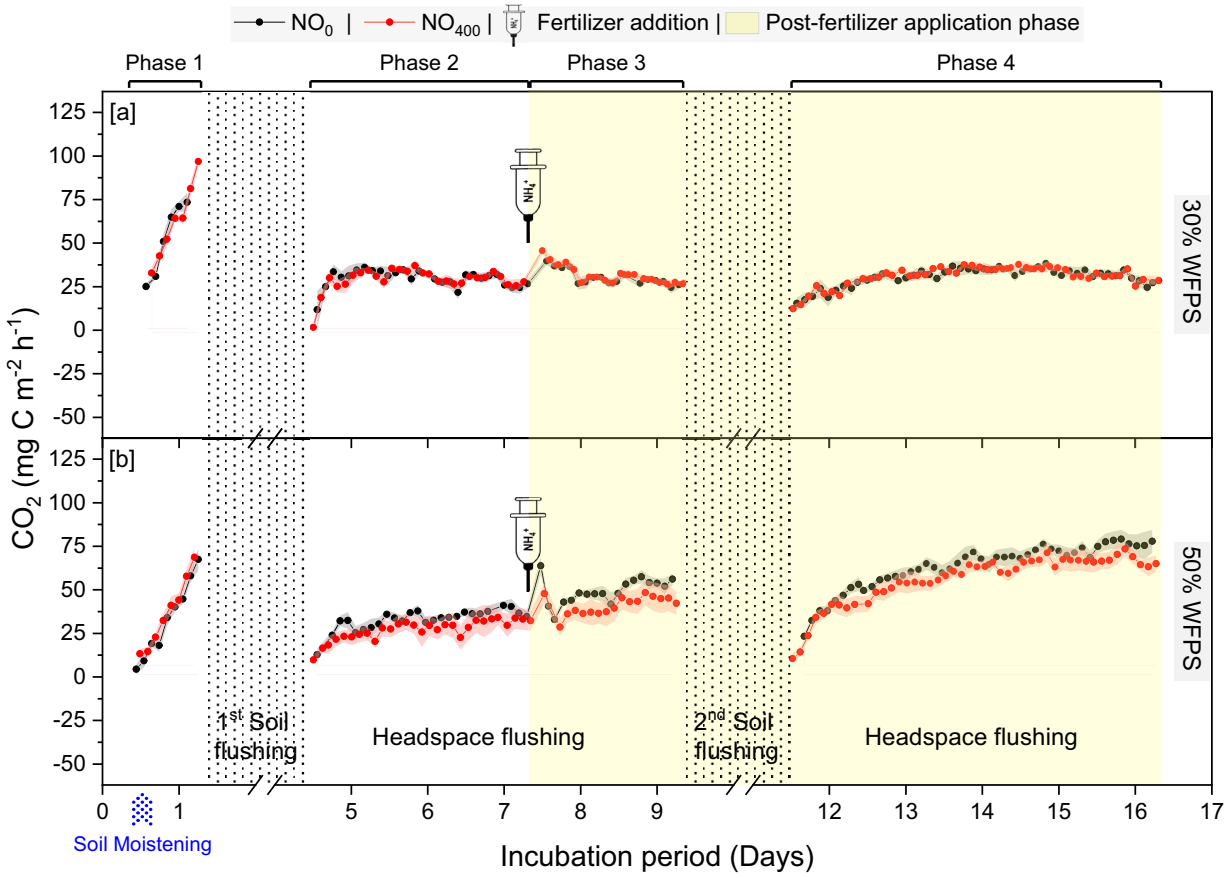

Fig. 4 Soil CO_2 fluxes affected by two different soil moisture levels (30% [**a**] and 50% [**b**] WFPS) and two different ambient NO concentrations (NO_0 and NO_{400}) used for soil and headspace flushing. Note: Vertical grey hashed columns indicate periods when soil surface fluxes could not be measured because the soil was flushed from below. Measurements are presented as mean ± standard error (SE) ($N = 6$)

Enrichment of the ambient air stream with NO (NO_{400}) reduced soil NO fluxes in most observational phases by > 10% compared to NO_0 (Table 2).

Soil NO_2 fluxes were at least one to two orders of magnitude lower than soil NO fluxes, with maximum emission fluxes of about 1.6 µg N m^{-2} h^{-1} (Fig. S3). Furthermore, Soil NO_2 fluxes were significantly lower for soils at 50% WFPS compared to soils at 30% WFPS. Spiking the ambient airflow with 400 ppbv NO (NO_{400}) reduced NO_2 fluxes by about 10% (Fig. S3, Table 2).

Rewetting of the air-dried soil to 50% WFPS resulted in a sharp increase in soil N_2O emissions towards the end of day 1 (up to 80 µg N m^{-2} h^{-1}), while for soils rewetted to 30% WFPS, no significant change in soil N_2O fluxes was observed, with fluxes < 5 µg N m^{-2} h^{-1}. N_2O fluxes from soils at 30% WFPS remained below 10 µg N m^{-2} h^{-1} throughout the observation period, even though the soils were fertilized on day 7. In contrast, N_2O fluxes from soils re-wetted to 50% WFPS peaked at about 120 µg N m^{-2} h^{-1} one week after fertilizer application.

For soils rewetted to 50% WFPS, soil N_2O fluxes were only marginally affected by differences in ambient air flow NO concentrations and a notable reduction in N_2O fluxes due to increased ambient NO concentrations was only observable for a short period of about 2 days immediately after N fertilization (Fig. 6, Table 2). With regard to soil N_2O fluxes for soils rewetted to 30%, the increased NO ambient air concentration resulted in reduced N_2O fluxes overall, but at a very low level.

Effect of soil moisture on ratios of soil N_2O:NO:NO_2 fluxes

Soil moisture affected the ratio of soil N trace gas fluxes. While at 30% WFPS NO fluxes were about 3–6 times higher as N_2O fluxes (N_2O:NO ratio: 0.14–0.31: 1) this relationship changed to the opposite at soil moisture contents of 50% WFPS (N_2O:NO ratio: 1.3–15.3: 1). CO_2:N_2O ratios were in the range of about 500–30000: 1, and were highest directly in the first phase of the experiment, i.e. after re-wetting to

Table 2 Cumulative N and C trace gas fluxes (mean ± SE, unit mg N or C m^{-2}) and trace gas ratios for different experimental phases

Gas species	%WFPS	Experimental phase (Days)		Phase 1 (0-1)	Phase 2 (5-7.5)	Phase 3 (7.5-9)	Phase 4 (12-17)	∑Phase 1-4 (0-17)
NO	30	NO_0		0.15 ± 0.01 ↓	4.30 ± 0.18 ↓	4.98 ± 0.24 ↓	9.70 ± 2.0	19.1 ± 2.1 ↓
		NO_{400}		0.13 ± 0.01	3.76 ± 0.21	4.40 ± 0.23	9.73 ± 1.06	18.0 ± 1.6
	50	NO_0		0.02 ± 0.03 ↑	0.69 ± 0.10 ↓	1.29 ± 0.16 ↓	4.82 ± 0.44 ↓	6.8 ± 0. 7 ↓
		NO_{400}		0.06 ± 0.09	0.58 ± 0.19	1.00 ± 0.10	4.22 ± 0.17	5.9 ± 0.2
N_2O	30	NO_0		0.05 ± 0.02 ↓	0.93 ± 0.11 ↓	0.67 ± 0.10 ↓	1.96 ± 0.11	3.6 ± 0.3 ↓
		NO_{400}		0.04 ± 0.02	0.78 ± 0.04	0.53 ± 0.04	1.82 ± 0.08	3.2 ± 0.1
	50	NO_0		0.35 ± 0.23	1.62 ± 0.31	1.70 ± 0.27	11.2 ± 2.5	14.9 ± 2.6
		NO_{400}		0.35 ± 0.12	1.54 ± 0.34	1.23 ± 0.26 ↓	11.6 ± 2.7	14.7 ± 3.2
NO_2	30	NO_0		0.0 ± 0.0	0.020 ± 0.001 ↓	0.05 ± 0.00 ↓	0.10 ± 0.02 ↓	0.17 ± 0.02 ↓
		NO_{400}		0.0 ± 0.0	0.016 ± 0.001 ↓	0.04 ± 0.00 ↓	0.08 ± 0.02 ↓	0.14 ± 0.02 ↓
	50	NO_0		0.0 ± 0.0	0.002 ± 0.001 ↓	0.01 ± 0.00 ↓	0.09 ± 0.01	0.10 ± 0.01
		NO_{400}		0.0 ± 0.0	0.001 ± 0.001 ↓	0.01 ± 0.00 ↓	0.09 ± 0.00	0.09 ± 0.00
CO_2	30	NO_0		1506 ± 754 ↓	2315 ± 222 ↓	1473 ± 51	3484 ± 162	8778 ± 773 ↓
		NO_{400}		1066 ± 102	2073 ± 39	1487 ± 93	3613 ± 66	8239 ± 124
	50	NO_0		741 ± 54 ↑	2202 ± 203 ↓	2229 ± 58 ↓	7010 ± 339	12182 ± 492
		NO_{400}		839 ± 95	1932 ± 353	1840 ± 283	6398 ± 403	11010 ± 1015
CH_4	30	NO_0		-0.01 ± 0.07	-0.01 ± 0.15 ↓	-0.01 ± 0.12 ↑	0.01 ± 0.11 ↓	-0.01 ± 0.34 ↑
		NO_{400}		-0.01 ± 0.07	-0.00 ± 0.16	-0.02 ± 0.12	-0.00 ± 0.16	-0.03 ± 0.37
	50	NO_0		0.01 ± 0.21 ↓	-0.37 ± 0.44 ↓	-0.01 ± 0.11 ↑	-0.11 ± 0.450 ↓	-0.48 ± 0.60 ↓
		NO_{400}		-0.03 ± 0.21	0.08 ± 0.24	-0.02 ± 0.07	-0.06 ± 0.49	-0.02 ± 0.53
Trace gas ratios								
Ratio	30	NO_0	CO_2:N_2O	30584:1	2485:1	2191:1	1782:1	2432:1
			CO_2:NO	9802:1	539:1	296:1	359:1	459:1
			N_2O:NO	0.3:1	0.2:1	0.1:1	0.2:1	0.2:1
		NO_{400}	CO_2:N_2O	26138:1	2653:1	2783:1	1984:1	2593:1
			CO_2:NO	8077:1	551:1	338:1	372:1	457:1
			N_2O:NO	0.3:1	0.2:1	0.1:1	0.2:1	0.2:1
Ratio	50	NO_0	CO_2:N_2O	2106:1	1362:1	1309:1	625:1	819:1
			CO_2:NO	32203:1	3202:1	1729:1	1454:1	1786:1
			N_2O:NO	15.3:1	2.4:1	1.3:1	2.3:1	2.2:1
		NO_{400}	CO_2:N_2O	2396:1	1254:1	1496:1	551:1	747:1
			CO_2:NO	14372:1	3341:1	1836:1	1517:1	1880:1
			N_2O:NO	6.0:1	2.7:1	1.2:1	2.8:1	2.5:1

*For the different experimental phases see e.g. Figure 4. Up and down arrows indicate ± 10% changes in mean trace gas fluxes comparing NO_{400} with control NO_0

the target soil moisture. Changes in ambient NO concentration did not affect the N_2O:NO, CO_2:N_2O or CO_2:NO ratios (Table 2).

Discussion

Automated soil mesocosm system for identifying drivers of soil C and N trace gas fluxes

While several soil mesocosm systems have been developed in the past to study and parameterize soil trace gas fluxes (e.g. Ausma et al. 2003; Capooci et al. 2019; Janz et al. 2022; Krause et al. 2017), we are not aware of a system like ours that allows to dynamically change the composition of the incoming airflow, e.g. to spiking the ambient airflow with NO as in our experiments and to measure changes in soil-atmosphere exchange rates of trace gases with such precision and accuracy. The developed mesocosm system is based on a previous version described earlier (Arias-Navarro et al. 2017), but has significant advantages regarding the control of air flows by flow controllers, the possibility of both soil and headspace flushing, or the simultaneous measurement of C and N trace gas fluxes with only one state-of-the-art quantum cascade laser instrument. The latter not only allowed us to measure trace gas concentrations with the highest precision but also to simplify and automate flux calculations using a standardized, customized R script, which was key for quality assurance and control of measurements. In addition, the system allowed us to monitor soil C and N trace gas fluxes from 12 mesocosms with high temporal resolution (length of measurement cycle for all 12 soil mesocosms 144 min), which is a prerequisite for observing short-term responses of soil-atmosphere trace gas flux changes, e.g. in response to rewetting, fertilization or changes in gas composition (e.g. Butterbach-Bahl et al. 2004; De Rosa et al. 2018; Wang et al. 2011).

Effects of soil moisture and fertilizer application on soil C and N trace gas fluxes

In agreement with many previous studies (Kechavarzi et al. 2010; Schindlbacher et al. 2004; Wu et al. 2017), pronounced effects of soil moisture changes on CO_2, N_2O, and NO fluxes and trace gas flux ratios were observed. In our experiments, initial soil re-wetting triggered a peak in soil respiration, which can be explained by the Birch effect, i.e. the rapid mineralization of easily degradable organic carbon substances originating from dead microbial biomass or in response to osmotic stress (Leitner et al. 2017a; Moyano et al. 2013; Unger et al. 2010). A pulse of N_2O emissions after rewetting was also detected, although delayed by about 8–10 h compared to CO_2 and only for soils rewetted to 50% WFPS, but not for NO. The latter is surprising, as the few available field and laboratory datasets reporting changes in

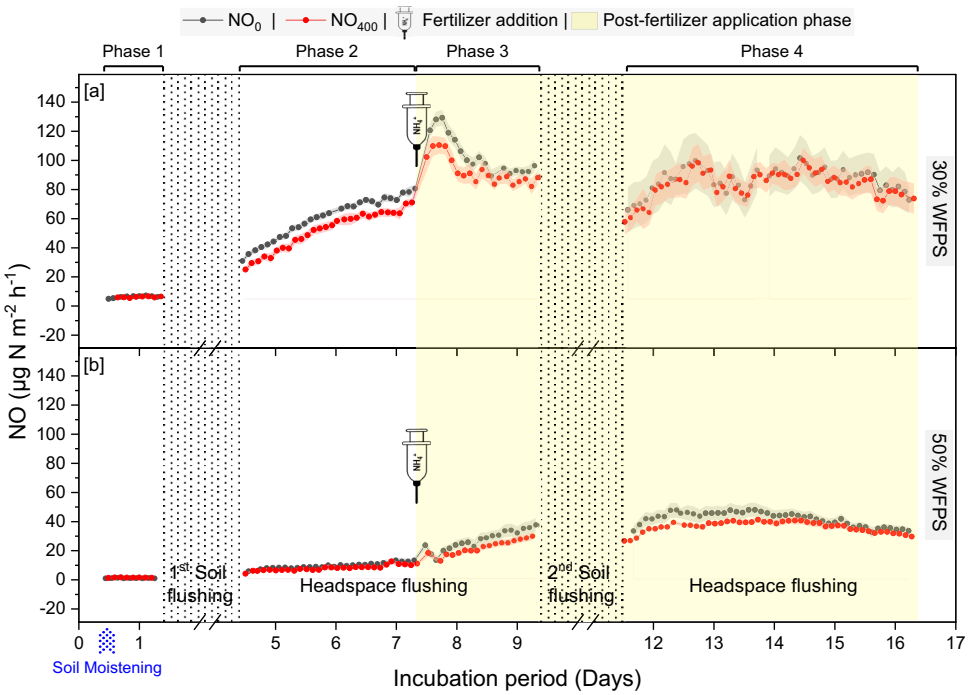

Fig. 5 Soil NO fluxes affected by two different soil moisture levels (30% [**a**] and 50% [**b**] WFPS) and two different ambient NO concentrations (NO_0 and NO_{400}) used for soil and headspace flushing. Note: Vertical grey hashed colums indicate periods when soil surface fluxes could not be measured because the soil was flushed from below. Measurements are presented as mean ± standard error (SE) ($N = 6$)

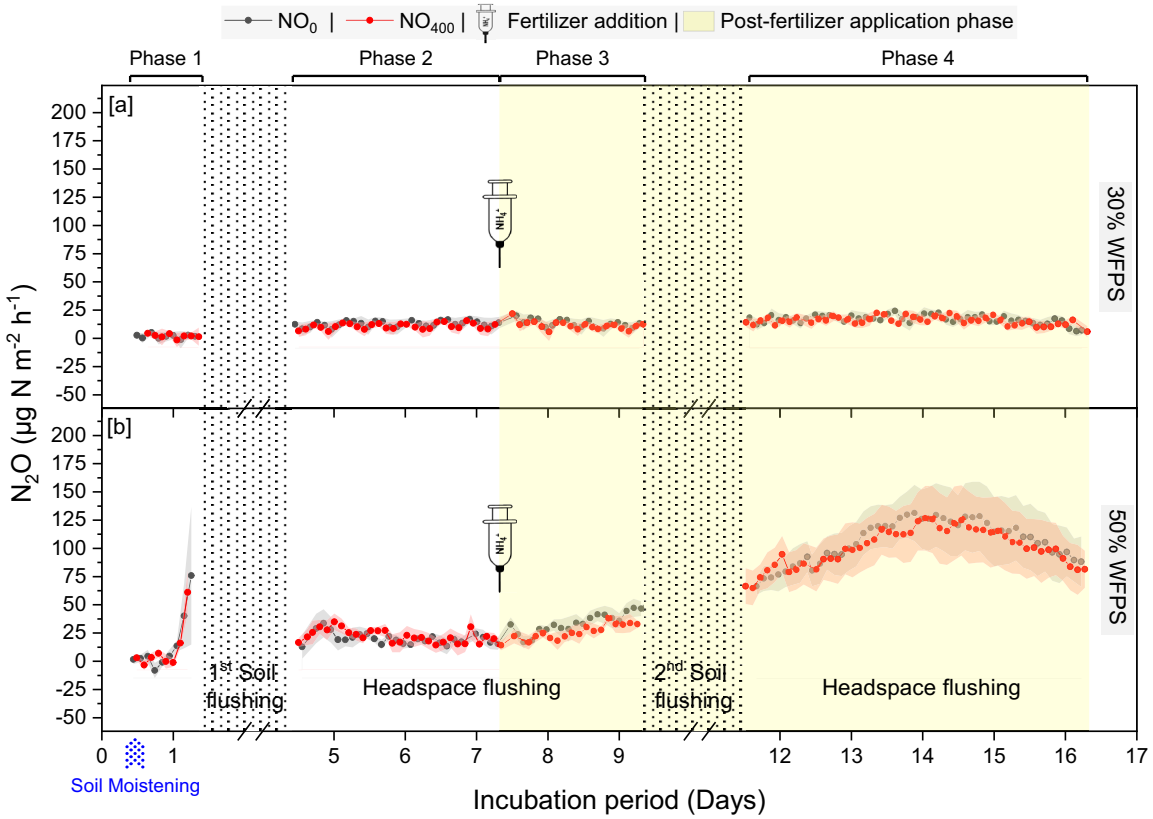

Fig. 6 Soil N_2O fluxes affected by two different soil moisture levels (30% [**a**] and 50% [**b**] WFPS) and two different ambient NO concentrations (NO_0 and NO_{400}) used for soil and headspace flushing. Note: Vertical grey hashed colums indicate periods when soil surface fluxes could not be measured because the soil was flushed from below. Measurements are presented as mean ± standard error (SE) ($N = 6$)

soil NO and N_2O fluxes after re-wetting report simultaneous stimulation of both N trace gas fluxes (Butterbach-Bahl et al. 2004; Hickman et al. 2021; Leitner et al. 2017b; Senbayram et al. 2022). We assume that the NO peak may be masked by the first soil gas flushing period, although this still implies that the rewetting N_2O flux pulse starts before a possible pulse in NO fluxes. Please also note that the results may be soil-type specific, depending on the phenotypic potential of the microbial community, and that the expression of N_2O reductase is delayed at higher availability of N-oxide substrates, including NO (e.g. Highton et al. 2022).

Over the entire 17-day experiment, CO_2 and N_2O fluxes were about 25% and 500% higher at 50% WFPS compared to 30% WFPS, about the same for CH_4, but about 60% lower for NO (Table 2). Soil respiration is known to be stimulated up to an optimum with increasing soil moisture as long as O_2 availability is not limited by gas diffusion limitations (Linn and Doran 1984; Manzoni et al. 2012). However, the optimum soil moisture for microbial activity is dependent on soil properties such as texture and organic matter content (Setia et al. 2011), and climate history (Evans et al. 2022). The strong stimulation of N_2O fluxes in the soil re-wetted to 50% WFPS, while NO fluxes were strongly reduced compared to soils re-wetted to 30% WFPS, indicates that at 50% WFPS, anaerobic microsites developed in the soils used in our experiments and that likely coupled nitrification–denitrification processes were occurring (Butterbach-Bahl et al. 2013). The observed N_2O:NO ratio as well as CO_2:N_2O and CO_2:NO ratios were in the range of 0.1–0.3:1, 550–30000:1, and 300–32000:1, respectively (Table 2). Such wide ranges of trace gas ratios and their dynamic changes in response to re-wetting have also been observed in field and laboratory studies (e.g. Butterbach-Bahl et al. 2004; Wang et al. 2013), Despite the limited number of studies, only a select few have reported on simultaneous measurements of CO_2, N_2O, and NO fluxes from soils. Most striking is the change in the N_2O:NO ratio from 0.2:1 for soils re-wetted to 30% WFPS to 2.2–2.5: 1 for soils re-wetted to 50% WFPS. This indicates that most likely nitrification was the dominant process for N trace gas production in soils re-wetted to 30% WFPS, whereas denitrification may have been the dominant process for N trace gas production (and consumption in the case of NO) at the higher soil moisture (Skiba et al. 1992; Yao et al. 2019). However, since NO is an intermediate in the nitrification process, the change in the N_2O:NO ratio may also be due to the production of N_2O by nitrification–denitrification (Stein 2019).

Fertilization of the soils resulted in an immediate increase in NO fluxes for the soils rewetted to 30%, whereas this was not observed for the wetter soil, although for this soil N_2O emissions eventually increased significantly a few days after fertilization (Figs. 5, and 6). Such significant differences in the response of NO and N_2O emissions to fertilization could be explained by the stimulation of anaerobic microsites in the soil due to the increased availability of inorganic N for microbial metabolism (Tian et al. 2020; Wang et al. 2024), although this interpretation is not supported by our measurements of soil CO_2 respiration fluxes, which hardly changed in response to fertilization (Fig. 4).

Effects of background NO concentrations on C and N trace gas fluxes

To our knowledge, this is the first study to investigate the effect of different ambient NO concentrations on the fluxes of N_2O, NO, CO_2, and CH_4. The applied NO concentrations, either close to zero (< 10 ppbv NO for NO_0) or around 400 ppbv NO (NO_{400}), are representative of the range of NO concentrations in soil air as found in a study covering a whole year with measurements at sub-daily resolution for a forest soil stand in southern Germany (Medinets et al. 2019). NO is known to act as an important regulator of microbial functions, and in the context of this study, its importance in assisting microbes to adapt to anaerobic conditions, in biofilm formation, or inhibiting nitrite-oxidizing bacteria (Courtens et al. 2015; Medinets et al. 2015) is likely to be the most important, as such effects can be traced to changes in soil C and N trace gas fluxes. When comparing NO_0 and NO_{400}, a decrease in soil C and N trace gas fluxes was observed in most cases and during all phases, except the first phase of soil rewetting. However, these effects remained insignificant due to the variability of the effects between soil mesocosms and the rather small changes in fluxes observed, which were in the range of -10 **to** -20%. Nevertheless, our results suggest that elevated soil NO concentrations negatively affect microbial respiration, CH_4 oxidation, and NO and N_2O emissions, but definitive proof of such a negative effect will require additional longer-duration experiments with a higher number of replicates, although our experiments were already run with six replicates.

Conclusion

We have successfully developed and tested a mesocosm system that can be used to automatically measure small changes in soil-atmosphere trace gas fluxes with high temporal resolution as a function of ambient air background concentrations, in order to better understand the controls on soil microbial processes or how pollutants may affect them. While we did not find significant effects of elevated background NO concentrations on soil C and N trace gas fluxes, still there was a tendency for fluxes to decrease at elevated NO concentrations, probably due to reduced microbial activity in the soil. Further experiments, including plants and vital rhizosphere activity, are needed to confirm potential effects.

Supplementary Information The online version contains supplementary material available at https://doi.org/10.1007/s00374-024-01862-5.

Acknowledgements This study was undertaken as part of the Franco-German Project NO-PIMS "What is the role of exogenous NO for plants, microbes, and their interactions in soil?". The project was supported financially by the Deutsche Forschungsgemeinschaft (DFG) of Germany (BU 1173/25-1) and the Agence Nationale de la Recherche (ANR) of France. KBB received additional funding from the Pioneer Center for Research in Sustainable Agricultural Futures (LandCRAFT), DNRF grant number P2.

Authors' contributions K.B.B., M.D., L.P., N.B., and L.S. designed the study, L.S., F.E., and B.W. built the mesocosm system, adapted the software, developed the data scripts and executed the experimented; K.B.B. and L.S. with support of all authors wrote the manuscript. All authors discussed the results and contributed to the final document. Funding acquisition by K.B.B., M.D., L.P., and N.B.

Funding Open Access funding enabled and organized by Projekt DEAL.

Data availability The datasets generated during and/or analyzed during the current study are available from the corresponding author upon reasonable request.

Declarations

Competing interests Declaration of absence of any competing interests or conflicts of interest among the authors.

References

Arias-Navarro C, Díaz-Pinés E, Zuazo P, Rufino MC, Verchot LV, Butterbach-Bahl K (2017) Quantifying the contribution of land use to N_2O, NO and CO_2 fluxes in a montane forest ecosystem of Kenya. Biogeochemistry 134:95–114. https://doi.org/10.1007/s10533-017-0348-3

Arruebarrena Di Palma AM, Pereyra C, Moreno Ramirez L, Xiqui Vázquez ML, Baca BE, Pereyra MA, Lamattina L, Creus CM (2013) Denitrification-derived nitric oxide modulates biofilm formation in Azospirillum brasilense. FEMS Microbiol Lett 338:77–85. https://doi.org/10.1111/1574-6968.12030

Ausma S, Edwards GC, Gillespie TJ (2003) Laboratory-scale measurement of trace gas fluxes from landfarm soils. J Environ Qual 32:8–22. https://doi.org/10.2134/jeq2003.8000

Butterbach-Bahl K, Gasche R, Breuer L, Papen H (1997) Fluxes of NO and N_2O from temperate forest soils: Impact of forest type, N deposition and of liming on the NO and N_2O emissions. Nutr Cycl Agroecosyst 48:79–90. https://doi.org/10.1023/a:1009785521107

Butterbach-Bahl K, Kock M, Willibald G, Hewett B, Buhagiar S, Papen H, Kiese R (2004) Temporal variations of fluxes of NO, NO_2, N_2O, CO_2, and CH_4 in a tropical rain forest ecosystem. Glob Biogeochem Cycles 18:1–11. https://doi.org/10.1029/2004GB002243

Butterbach-Bahl K, Baggs EM, Dannenmann M, Kiese R, Zechmeister-Boltenstern S (2013) Nitrous oxide emissions from soils: how well do we understand the processes and their controls? Phil Trans R Soc B 368:20130122. https://doi.org/10.1098/rstb.2013.0122

Capooci M, Barba J, Seyfferth AL, Vargas R (2019) Experimental influence of storm-surge salinity on soil greenhouse gas emissions from a tidal salt marsh. Sci Total Environ 686:1164–1172. https://doi.org/10.1016/j.scitotenv.2019.06.032

Courtens ENP, De Clippeleir H, Vlaeminck SE, Jordaens R, Park H, Chandran K, Boon N (2015) Nitric oxide preferentially inhibits nitrite oxidizing communities with high affinity for nitrite. J Biotechnol 193:120–122. https://doi.org/10.1016/j.jbiotec.2014.11.021

De Rosa D, Rowlings DW, Biala J, Scheer C, Basso B, Grace PR (2018) N_2O and CO_2 emissions following repeated application of organic and mineral N fertiliser from a vegetable crop rotation. Sci Total Environ 637–638:813–824. https://doi.org/10.1016/j.scitotenv.2018.05.046

Eugster W, Merbold L (2015) Eddy covariance for quantifying trace gas fluxes from soils. Soil 1:187–205. https://doi.org/10.5194/soil-1-187-2015

Evans S, Allison SD, Hawkes CV (2022) Microbes, memory and moisture: Predicting microbial moisture responses and their impact on carbon cycling. Funct Ecol 36:1430–1441. https://doi.org/10.1111/1365-2435.14034

Gao F, Yates SR (1998) Laboratory study of closed and dynamic flux chambers: Experimental results and implications for field application. J Geophys Res Atmos 103:26115–26125. https://doi.org/10.1029/98JD01346

Gaupels F, Kuruthukulangarakoola GT, Durner J (2011) Upstream and downstream signals of nitric oxide in pathogen defence. Curr Opin Plant Biol 14:707–714. https://doi.org/10.1016/j.pbi.2011.07.005

Gusarov I, Shatalin K, Starodubtseva M, Nudler E (2009) Endogenous nitric oxide protects bacteria against a wide spectrum of antibiotics. Science 325:1380–1384. https://doi.org/10.1126/science.1175439

Harazono Y, Iwata H, Sakabe A, Ueyama M, Takahashi K, Nagano H, Nakai T, Kosugi Y (2015) Effects of water vapor dilution on trace gas flux, and practical correction methods. J Agric Meteorol 71:65–76. https://doi.org/10.2480/agrmet.D-14-00003

Hickman JE, Kaya B, Kebede A, Kandji S, Fitch L, Neill C, Nyadzi G, Diru W, Palm CA (2021) Little effect of land use on N_2O and NO emission pulses following rewetting of dry soils across seasonally dry sub-Saharan Africa. J Geophys Res Biogeosci 126:1–18. https://doi.org/10.1029/2020JG005742

Highton MP, Bakken LR, Dörsch P, Molstad L, Morales SE (2022) Nitrite accumulation and impairment of N_2O reduction explains contrasting soil denitrification phenotypes. Soil Biol Biochem 166:108529. https://doi.org/10.1016/j.soilbio.2021.108529

Hogewoning SW, Wientjes E, Douwstra P, Trouwborst G, van Ieperen W, Croce R, Harbinson J (2012) Photosynthetic quantum yield dynamics: from photosystems to leaves. Plant Cell 24:1921–1935. https://doi.org/10.1105/tpc.112.097972

IUSS Working Group WRB (2022) World reference base for soil resources. International soil classification system for naming soils and creating legends for soil maps. International Union of Soil Sciences (IUSS), 4th edn. Vienna, Austria

Janz B, Havermann F, Lashermes G, Zuazo P, Engelsberger F, Torabi SM, Butterbach-Bahl K (2022) Effects of crop residue incorporation and properties on combined soil gaseous N_2O, NO, and NH_3 emissions—A laboratory-based measurement approach. Sci Total Environ Part 2(807):151051. https://doi.org/10.1016/j.scitotenv.2021.151051

Jeandroz S, Lamotte O, Astier J, Rasul S, Trapet P, Besson-Bard A, Bourque S, Nicolas-Francès V, Ma W, Berkowitz GA, Wendehenne D (2013) There's more to the picture than meets the

eye: Nitric oxide cross talk with Ca^{2+} signaling. Plant Physiol 163:459–470. https://doi.org/10.1104/pp.113.220624

Kechavarzi C, Dawson Q, Bartlett M, Leeds-Harrison PB (2010) The role of soil moisture, temperature and nutrient amendment on CO_2 efflux from agricultural peat soil microcosms. Geoderma 154:203–210. https://doi.org/10.1016/j.geoderma.2009.02.018

Koul V, Adholeya A, Kochar M (2015) Sphere of influence of indole acetic acid and nitric oxide in bacteria. J Basic Microbiol 55:543–553. https://doi.org/10.1002/jobm.201400224

Krause HM, Thonar C, Eschenbach W, Well R, Mäder P, Behrens S, Kappler A, Gattinger A (2017) Long term farming systems affect soils potential for N_2O production and reduction processes under denitrifying conditions. Soil Biol Biochem 114:31–41. https://doi.org/10.1016/j.soilbio.2017.06.025

Leitner S, Homyak PM, Blankinship JC, Eberwein J, Jenerette GD, Zechmeister-Boltenstern S, Schimel JP (2017a) Linking NO and N_2O emission pulses with the mobilization of mineral and organic N upon rewetting dry soils. Soil Biol Biochem 115:461–466. https://doi.org/10.1016/j.soilbio.2017.09.005

Leitner S, Minixhofer P, Inselsbacher E, Keiblinger KM, Zimmermann M, Zechmeister-Boltenstern S (2017b) Short-term soil mineral and organic nitrogen fluxes during moderate and severe drying–rewetting events. Appl Soil Ecol 114:28–33. https://doi.org/10.1016/j.apsoil.2017.02.014

Linn DM, Doran JW (1984) Effect of water-filled pore space on carbon dioxide and nitrous oxide production in tilled and nontilled soils. Soil Sci Soc Am J 48:1267–1272. https://doi.org/10.2136/sssaj1984.03615995004800060013x

Ma M, Wendehenne D, Philippot L, Hänsch R, Flemetakis E, Hu B, Rennenberg H (2020) Physiological significance of pedospheric nitric oxide for root growth, development and organismic interactions. Plant Cell Environ 43:2336–2354. https://doi.org/10.1111/pce.13850

Manzoni S, Schimel JP, Porporato A (2012) Responses of soil microbial communities to water stress: Results from a meta-analysis. Ecology 93:930–938. https://doi.org/10.1890/11-0026.1

Medinets S, Skiba U, Rennenberg H, Butterbach-Bahl K (2015) A review of soil NO transformation: Associated processes and possible physiological significance on organisms. Soil Biol Biochem 80:92–117. https://doi.org/10.1016/j.soilbio.2014.09.025

Medinets S, Gasche R, Kiese R, Rennenberg H, Butterbach-Bahl K (2019) Seasonal dynamics and profiles of soil NO concentrations in a temperate forest. Plant Soil 445:335–348. https://doi.org/10.1007/s11104-019-04305-5

Moyano FE, Manzoni S, Chenu C (2013) Responses of soil heterotrophic respiration to moisture availability: An exploration of processes and models. Soil Biol Biochem 59:72–85. https://doi.org/10.1016/j.soilbio.2013.01.002

Pape L, Ammann C, Nyfeler-Brunner A, Spirig C, Hens K, Meixner FX (2009) An automated dynamic chamber system for surface exchange measurement of non-reactive and reactive trace gases of grassland ecosystems. Biogeosciences 6:405–429. https://doi.org/10.5194/bg-6-405-2009

Pilegaard K (2013) Processes regulating nitric oxide emissions from soils. Philos Trans R Soc B 368:20130126. https://doi.org/10.1098/rstb.2013.0126

Privett BJ, Broadnax AD, Bauman SJ, Riccio DA, Schoenfisch MH (2012) Examination of bacterial resistance to exogenous nitric oxide. Nitric Oxide Biol Chem 26:169–173. https://doi.org/10.1016/j.niox.2012.02.002

Schairer DO, Chouake JS, Nosanchuk JD, Friedman AJ (2012) The potential of nitric oxide releasing therapies as antimicrobial agents. Virulence 3:271–279. https://doi.org/10.4161/viru.20328

Schindlbacher A, Zechmeister-Boltenstern S, Butterbach-Bahl K (2004) Effects of soil moisture and temperature on NO, NO_2, and N_2O emissions from European forest soils. J Geophys Res Atmos 109:1–12. https://doi.org/10.1029/2004JD004590

Schuster M, Conrad R (1992) Metabolism of nitric oxide and nitrous oxide during nitrification and denitrification in soil at different incubation conditions. FEMS Microbiol Lett 101:133–143. https://doi.org/10.1111/j.1574-6968.1992.tb05769.x

Senbayram M, Wei Z, Wu D, Shan J, Yan X, Well R (2022) Inhibitory effect of high nitrate on N_2O reduction is offset by long moist spells in heavily N loaded arable soils. Biol Fertil Soils 58:77–90. https://doi.org/10.1007/s00374-021-01612-x

Setia R, Marschner P, Baldock J, Chittleborough D, Verma V (2011) Relationships between carbon dioxide emission and soil properties in salt-affected landscapes. Soil Biol Biochem 43:667–674. https://doi.org/10.1016/j.soilbio.2010.12.004

Skiba U, Hargreaves KJ, Fowler D, Smith KA (1992) Fluxes of nitric and nitrous oxides from agricultural soils in a cool temperate climate. Atmos Environ Part A 26:2477–2488. https://doi.org/10.1016/0960-1686(92)90100-Y

Spiro S (2007) Regulators of bacterial responses to nitric oxide. FEMS Microbiol Rev 31:193–211. https://doi.org/10.1111/j.1574-6976.2006.00061.x

Stein LY (2019) Insights into the physiology of ammonia-oxidizing microorganisms. Curr Opin Chem Biol 49:9–15. https://doi.org/10.1016/j.cbpa.2018.09.003

Tian D, Zhang Y, Mu Y, Liu J, He K (2020) Effect of N fertilizer types on N_2O and NO emissions under drip fertigation from an agricultural field in the North China Plain. Sci Total Environ 715:136903. https://doi.org/10.1016/j.scitotenv.2020.136903

Unger S, Máguas C, Pereira JS, David TS, Werner C (2010) The influence of precipitation pulses on soil respiration - Assessing the " Birch effect" by stable carbon isotopes. Soil Biol Biochem 42:1800–1810. https://doi.org/10.1016/j.soilbio.2010.06.019

Wang R, Willibald G, Feng Q, Zheng X, Liao T, Brüggemann N, Butterbach-Bahl K (2011) Measurement of N_2, N_2O, NO, and CO_2 emissions from soil with the gas-flow-soil-core technique. Environ Sci Technol 45:6066–6072. https://doi.org/10.1021/es1036578

Wang R, Feng Q, Liao T, Zheng X, Butterbach-Bahl K, Zhang W, Jin C (2013) Effects of nitrate concentration on the denitrification potential of a calcic cambisol and its fractions of N_2, N_2O and NO. Plant Soil 363:175–189. https://doi.org/10.1007/s11104-012-1264-x

Wang Y, Yao Z, Pan Z, Guo H, Chen Y, Cai Y, Zheng X (2024) Nonlinear response of soil nitric oxide emissions to fertilizer nitrogen across croplands. Biol Fertil Soils 60:483–492. https://doi.org/10.1007/s00374-024-01818-9

Webb EK, Pearman GI, Leuning R (1980) Correction of flux measurements for density effects due to heat and water vapour transfer. Q J R Meteorol Soc 106:85–100. https://doi.org/10.1002/qj.49710644707

Weber P, Rennenberg H (1996) Exchange of NO and NO_2 between wheat canopy monoliths and the atmosphere. Plant Soil 180:197–208. https://doi.org/10.1007/BF00015303

Wendehenne D, Gao Q, Ming Kachroo A, Kachroo P (2014) Free radical-mediated systemic immunity in plants. Curr Opin Plant Biol 20:127–134. https://doi.org/10.1016/j.pbi.2014.05.012

Wu D, Cárdenas LM, Calvet S, Brüggemann N, Loick N, Liu S, Bol R (2017) The effect of nitrification inhibitor on N_2O, NO and N_2 emissions under different soil moisture levels in a permanent grassland soil. Soil Biol Biochem 113:153–160. https://doi.org/10.1016/j.soilbio.2017.06.007

Yao Z, Zheng X, Wang R, Liu C, Lin S, Butterbach-Bahl K (2019) Benefits of integrated nutrient management on N_2O and NO mitigations in water-saving ground cover rice production systems. Sci Total Environm 646:1155–1163. https://doi.org/10.1016/j.scitotenv.2018.07.393

Yu J, Meixner FX, Sun W, Liang Z, Chen Y, Mamtimin B, Wang G, Sun Z (2008) Biogenic nitric oxide emission from saline sodic

soils in a semiarid region, northeastern China: A laboratory study. J Geophys Res Biogeosci 113:1–11. https://doi.org/10.1029/2007JG000576

Yu M, Lamattina L, Spoel SH, Loake GJ (2014) Nitric oxide function in plant biology: A redox cue in deconvolution. New Phytol 202:1142–1156. https://doi.org/10.1111/nph.12739